

Inferring the mesoscale structure of layered, edge-valued and time-varying networks

Tiago P. Peixoto*

Institut für Theoretische Physik, Universität Bremen, Hochschulring 18, D-28359 Bremen, Germany

Many network systems are composed of interdependent but distinct types of interactions, which cannot be fully understood in isolation. These different types of interactions are often represented as layers, attributes on the edges or as a time-dependence of the network structure. Although they are crucial for a more comprehensive scientific understanding, these representations offer substantial challenges. Namely, it is an open problem how to precisely characterize the large or mesoscale structure of network systems in relation to these additional aspects. Furthermore, the direct incorporation of these features invariably increases the effective dimension of the network description, and hence aggravates the problem of overfitting, i.e. the use of overly-complex characterizations that mistake purely random fluctuations for actual structure. In this work, we propose a robust and principled method to tackle these problems, by constructing generative models of modular network structure, incorporating layered, attributed and time-varying properties, as well as a nonparametric Bayesian methodology to infer the parameters from data and select the most appropriate model according to statistical evidence. We show that the method is capable of revealing hidden structure in layered, edge-valued and time-varying networks, and that the most appropriate level of granularity with respect to the additional dimensions can be reliably identified. We illustrate our approach on a variety of empirical systems, including a social network of physicians, the voting correlations of deputies in the Brazilian national congress, the global airport network, and a proximity network of high-school students.

I. INTRODUCTION

The network abstraction has been successfully used as a powerful framework behind the modeling of a great variety of biological, technological and social systems [1]. Traditionally, most network models proposed in these contexts consist of a set of elements possessing a single type of pairwise interaction (e.g. epidemic contact, transport route, metabolic reaction, etc.). More recently, it has become increasingly clear that single types of interaction do not occur in isolation, and that a complete system encompasses several layers of interactions [2–4], and very often change in time [5]. Many examples have shown that the interplay between different types of interactions can dramatically change the outcome of paradigmatic processes such as percolation [6], epidemic spreading [7–9], diffusion [10, 11], opinion formation [12–14], evolutionary games [15–17], and synchronization [3, 18], among others. The realization that different types of interaction need to be incorporated into network models also changes the way data need to be analyzed. In particular, the large or mesoscale structure of network systems may be intertwined with the layered or temporal structure, in such a way that cannot be visible if this information is omitted. The conventional approach of representing mesoscale structures is to separate the nodes into groups (or modules, “communities”) that have a similar role in the network topology [19]. Some methods have been proposed to identify such groups in both layered [4, 20–22] and time-varying [20, 21, 23–28] networks. However, these methods do not address two very

central questions: 1. Is the layered or temporal structure indeed important for the description of the network? And if so, to what degree of granularity? 2. How does one distinguish between multiple descriptions of the same network, and in particular separate actual structure from stochastic fluctuations? In this work we tackle both these questions by formulating generative models of layered networks, obtained by generalizing several variants of the stochastic block model [29–32], incorporating features such as hierarchical structure [33, 34], overlapping groups [35–37] and degree-correction [38], in addition to different types of layered structure. We show how the unsuspecting incorporation of many layers that happen to be uncorrelated with the mesoscale structure can in fact hinder the detection task, and obscure structure that would be visible by ignoring the layer division in the usual fashion. Since most methods proposed so far take any available layer information for granted, and attempt to model it in absolute detail, this issue represents a severe limitation of these methods in capturing the structure of layered networks in a reliable manner. We show how this problem can be solved by performing model selection under a general nonparametric Bayesian framework, that can also be used to select between different model flavors (e.g. with overlapping groups or degree correction). We demonstrate that the proposed methodology can also be used to infer mesoscale structure in networks with real-valued correlates on the edges (such as weights, distances, etc.), while reliably distinguishing structure from noise, as well as change-points in time varying networks [39].

This work extends recent developments on layered [40–45], edge-valued [46–49] and temporal [50–54] generative processes, not only by incorporating many important topological patterns simultaneously (i.e. hierarchical structure, degree correction and overlapping groups),

* tiago@itp.uni-bremen.de

but also by tying all these types of model into a nonparametric Bayesian framework that permits model selection, and avoids overfitting. The framework presented allows one not only to select among all different model classes, but also their appropriate order, i.e. the number of groups, layer bins and hierarchical structure. This is done in a principled fashion, based on statistical evidence and the principle of parsimony, and without the specification of *ad hoc* parameters. Furthermore, since it is based on the computation of posterior probabilities, it can be extended to other probabilistic models.

This paper is divided as follows. In Sec. II we formulate generative models for layered structure, including a very diverse set of possible topological patterns, and in Sec. III we describe a Bayesian model selection procedure to choose between them based on statistical evidence. In Sec. IV we tackle the problem of deciding whether or not the layered structure is informative of the network structure. In Sec. V we show how the layered models can be adapted to networks with real-valued edge-covariates, and in Sec. VI to networks that change in time, for which the division into layers corresponds to a detection of change-points. We finalize in Sec. VII with a conclusion.

II. GENERATIVE MODELS OF LAYERED NETWORKS

We consider graphs that have a layered structure [2, 3], so that the adjacency matrix in layer $l \in [1, C]$ can be written as A_{ij}^l (with values in the range $[0, 1]$ for a simple graph, or in \mathbb{N} for a multigraph), corresponding to the presence of an edge between vertices i and j in layer l . We will consider both directed and undirected graphs (i.e. A_{ij}^l being asymmetric and symmetric, respectively), although we will focus on the undirected case in most of the derivations, since the directed cases are mostly straightforward modifications (which are summarized in Appendix B). Here we assume that the vertices are globally indexed, and in principle can receive edges in all layers. The *collapsed graph* corresponds to the merging of all edges in a single layer, with a resulting adjacency matrix $A_{ij} = \sum_l A_{ij}^l$. In the following, we will denote a specific layered graph as $\{G_l\}$ (with $G_l = \{A_{ij}^l\}$ being an individual layer), and its corresponding collapsed graph as $G_c = \{A_{ij}\}$.

In this work we will consider two alternative ways of generating a given layered graph $\{G_l\}$ (see Fig. 1). The first approach interprets the layers as edge covariates [46]: First the collapsed graph G_c is generated, and then the layer membership of each edge is a random variable sampled from a distribution conditioned on the adjacent vertices. In the second approach, the graphs G_l at each layer l are generated independently from each other. (Henceforth we call these alternatives simply by “edge covariates” and “independent layers”, respectively). These different generative processes do not exhaust the realm of

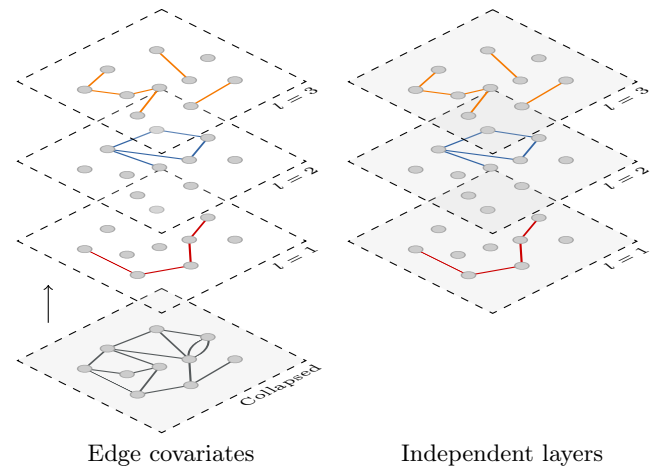


Figure 1. (Color online) Two processes capable of generating layered networks. *Left:* The collapsed graph is generated first, and conditioned on it, the edges are distributed among the layers. *Right:* The layers are formed independently from each other.

possible multilayer models. Instead, the objective here is to consider the most basic possibilities that allow us to incorporate different types of properties into the generated networks, and enable the formulation of a nonparametric model selection framework to decide if either one is more appropriate than the other depending on the statistical evidence available in the data, as discussed in detail below.

In the following we define two versions of the stochastic block model family (SBM), corresponding to the alternatives outlined above.

A. SBM with edge covariates

We generate first a collapsed graph from the traditional SBM ensemble, where N nodes are divided into B groups, via the membership vector $\{b_i\} \in [1, B]^N$, and the number of edges randomly placed between groups r and s is given by the edge counts e_{rs} (or twice the number if $r = s$, for convenience of notation). After the graph is generated, for each set of edges incident on groups r and s , we distribute the layer memberships randomly, conditioned only on the total number of edges of each type l between the two groups, m_{rs}^l . Any particular distribution of covariates among edges incident on groups r and s is generated with the same probability, which in the case of simple undirected graphs is given by

$$\frac{\prod_l m_{rs}^l!}{m_{rs}!}, \quad (1)$$

where $m_{rs} = \sum_l m_{rs}^l = (1 - \delta_{rs}/2)e_{rs}$. For the multigraph case, see Appendix A. If we use the shorthand $\{\theta\} = \{\{e_{rs}^l\}, \{b_i\}\}$ for the model parameters, the total

likelihood of observing the layered graph is

$$P(\{G_l\}|\{\theta\}) = P(G_c|\{\theta\}) \prod_{r \leq s} \frac{\prod_l m_{rs}^l!}{m_{rs}!}, \quad (2)$$

where $P(G_c|\{\theta\}) = e^{-S_t}$ is the likelihood of the collapsed stochastic block model, where S_t is the microcanonical entropy [55]. For instance, for simple undirected graphs that are sparse (i.e. with $e_{rs} \ll n_r n_s$), we have [55]

$$\mathcal{S}_t \approx E - \frac{1}{2} \sum_{rs} e_{rs} \ln \frac{e_{rs}}{n_r n_s}. \quad (3)$$

Here we are free to replace the traditional SBM by any other flavor, which amounts simply to a different likelihood in the first term of Eq. 2. The traditional SBM considered above imposes that all nodes belonging to the same group will receive the same number of edges on average, with little variation. An important alternative to this is the degree-corrected stochastic block model (DCSBM) [38], that includes as additional model parameters the degree sequence of the network, $\{k_i\}$. As argued in Ref. [38], and supported by an empirical model selection analysis in Ref. [37], this version is often a better model for many (collapsed) networks that feature significant degree variability. However, in this version with edge covariates, only the degrees of the *collapsed graph* are constrained, and thus the edges incident on a specific node will be distributed randomly among the layers independently of its degree. Hence, for networks generated in this manner, nodes with a large collapsed degree will also tend to possess uniformly larger degrees in all layers, when compared to other nodes of the same group with a lower collapsed degree. In other words, this model does not allow for degree variability *across layers*.

The complete likelihood of this model can be obtained in an entirely analogous fashion, simply by augmenting the parameter set in Eq. 2 to include the collapsed degree sequence, i.e. $\{\theta\} = \{\{e_{rs}^l\}, \{b_i\}, \{k_i\}\}$, and using the likelihood of the degree-corrected model [55].

Other useful variations are SBMs with mixed memberships (e.g. [35–37]), in which nodes are allowed to belong to more than one group. Here we use the formulation of Ref. [37], where we need to replace the node partitions above by overlapping partitions, $\{\vec{b}_i\}$, where \vec{b}_i determines the mixture of node i , with $b_i^r \in \{0, 1\}$ specifying whether node i belongs to group r , so that $\{\theta\} = \{\{\vec{b}_i\}, \{e_{rs}\}\}$. Likewise, for the degree-corrected version, we need to specify the (collapsed) labeled degree sequence $\{\vec{k}_i\}$, where k_i^r is the degree of node i of type r , leading to $\{\theta\} = \{\{\vec{b}_i\}, \{e_{rs}\}, \{\vec{k}_i\}\}$. In both cases we simply replace the likelihood in Eq. 2 by the ones described in Ref. [37].

B. SBM with independent layers

Alternatively, we may generate each layer as an independent SBM, constrained only by the fact that the

group memberships of the nodes are the same across all layers (although this can be relaxed in the overlapping version, as discussed below). Furthermore, we allow nodes to belong only to a subset of the layers, by including a $N \times C$ layer membership matrix $\{z_{il}\}$, where each binary entry $z_{il} \in [0, 1]$ determines whether node i belongs to layer l . If a node does not belong to a given layer, it is forbidden to receive edges of that type.

Using the shorthand $\{\{\theta\}_l\} = \{\{e_{rs}^l\}\}$ and $\{\phi\} = \{b_i\}$, the likelihood of the resulting layered block model is simply

$$P(\{G_l\}|\{\{\theta\}_l\}, \{\phi\}, \{z_{il}\}) = \prod_l P(G_l|\{\theta\}_l, \{\phi\}), \quad (4)$$

with $P(G_l|\{\theta\}_l, \{\phi\})$ being the likelihood of the traditional stochastic block model as before, where G_l is the subgraph containing only the edges of layer l and the nodes specified by $\{z_{il}\}$.

Like with the edge covariates model, here we are also free to replace the traditional SBM by any other flavor, which amounts simply to different likelihoods in the product of Eq. 4. However, differently from the SBM with edge covariates, if we wish to include degree correction, we need to specify the *layer-specific* degree sequence $\{k_i^l\}$, where $k_i^l = \sum_j A_{ij}^l$ is the degree of node i in layer l , so that $\{\{\theta\}_l\} = \{\{e_{rs}^l\}, \{k_i^l\}\}$. Therefore, unlike the previous case, this model allows for degree variability across different layers, i.e. a node with a large degree in one layer, may possess very low degree in another. Note that given the layer-specific degree sequence, we do not need to distinguish between nodes that belong or not to a layer, since a node with a layer-specific degree equal to zero will inherently not receive any edge in that layer. Therefore the parameters $\{k_i^l\}$ replace the parameters $\{z_{ij}\}$, which are removed from Eq. 4 in this case.

We again may wish to use mixed-membership models in each layer, by using overlapping partitions as parameters, i.e. $\{\phi\} = \{\vec{b}_i\}$. For the degree-corrected version, we need to specify the labeled degree sequence *at each layer*, $\{\vec{k}_i\}_l$, where k_i^r is the degree of node i of type r in layer l , i.e. $\{\{\theta\}_l\} = \{\{e_{rs}^l\}, \{\vec{k}_i\}_l\}$. We may view the labeled degree sequence inside each layer as a weighted membership to each group. Since these “weights” may change across the layers (even becoming zero), this corresponds to a generalization that allows the memberships to change arbitrarily between the layers (despite the fact that the overall, unweighted group mixtures $\{\vec{b}_i\}$ are constant across the layers). This is a particularly useful property for temporal networks, that allows group membership to change in time, as discussed in more detail in Sec. VI.

C. Equivalence between models

The “independent layers” and “edge covariates” models are equivalent in some situations, and different in others. In particular, in the non-degree-corrected case described above, if all nodes belong to all layers, both models generate the same networks asymptotically with the same probability. This can be seen by employing Stirling’s approximation $\ln e_{rs}^l \approx e_{rs}^l \ln e_{rs}^l - e_{rs}^l$ in Eq. 2, which makes it identical to Eq. 4. Hence, as long as the edge counts in each layer are sufficiently large, these models are fully equivalent. However, if nodes belong only to specific subset of the layers, these models are not equivalent. In this case, only the model with independent layers will take the heterogeneous layer memberships into account, and hence it should be preferred. Since we assume that the layer memberships are known *a priori* there is no reason to employ the “edge covariates” non-degree-corrected model, since the “independent layers” model will always provide an equal or better description asymptotically¹.

The situation is different for the degree-corrected models. Strictly, both model versions are not equivalent, since the layered version allows for degree variability across layers, whereas the covariate version does not. Hence, there are networks generated by the layered model that cannot be generated (or only with a vanishing probability) by the edge covariates model. The opposite, however, is not true: A layered network generated by the covariate version can always be sampled with the independent layers version given an appropriate parameter choice.

Since the SBM with independent layers version always encapsulates the edge covariate version, one might be tempted to prefer it systematically. However, one needs to realize that the layered version requires more parameters than the covariates version, either via the layer membership matrix $\{z_{il}\}$ or the layer-specific degree sequence $\{k_i^l\}$. Similar comparisons can be made between specific flavors of both models (e.g. with overlapping groups or degree correction). Because of the increased number of degrees of freedom in the model specification, we risk overfitting the data by always choosing the most constrained model. We discuss exactly how this choice between models should be done in the next section.

III. SELECTING THE MOST APPROPRIATE MODEL

The proper way to select between alternatives is to perform model selection based on statistical significance, and opt for the more complicated model only if there is sufficient evidence available in the data to compensate the larger number of parameters. Formulated in a

Bayesian setting, as proposed in Ref. [37], this selection procedure amounts to finding the model that maximizes the posterior likelihood

$$P(\{\theta\}|G_l) = \frac{P(\{G_l\}|\{\theta\})P(\{\theta\})}{P(\{G_l\})}, \quad (5)$$

where $\{\theta\}$ is a shorthand for the entire set of model parameters (e.g. for the non-degree-corrected SBM with edge covariates we have $\{\theta\} = \{b_i\}, \{e_{rs}^l\}$), $P(\{\theta\})$ is the prior probability on the parameters, and $P(\{G_l\})$ is a normalization constant. Since in our context we are dealing with discrete parameters, we can write $P(\{\theta\}) = e^{-\mathcal{L}(\{\theta\})}$, where $\mathcal{L}(\{\theta\})$ is the microcanonical entropy of the parameter ensemble. Therefore, we have that $-\ln P(\{\theta\}|G_l) = \Sigma + \ln P(\{G_l\})$ with $\Sigma = \mathcal{S}(\{G_l\}) + \mathcal{L}(\{\theta\})$ being the description length of the data [56–58]. Hence this approach amounts to finding the model that most compresses the observed data, i.e. the one with the minimum description length, since to maximize $P(\{\theta\}|G_l)$ is equivalent to minimize Σ [34, 37, 59].

Here we observe that since the prior probabilities are nonparametric, the whole procedure also becomes parameter-free, and hence no *ad hoc* choices are required *a priori*. In particular for the SBM variants considered in this work, the partition of the nodes, degree of overlap, the number of groups and the hierarchical structure are obtained in entirely nonparametric fashion.

A. Choice of priors

In order to compute $P(\{\theta\})$, we need to describe generative processes for the parameter themselves. This means that for the model variants above we need to specify a generative process for the partition into B groups $\{b_i\}$, the layer membership matrix $\{z_{il}\}$, the collapsed (or layer-specific) degree-sequence $\{k_i\}$ (or $\{k_i^l\}$), and the layered edge counts $\{e_{rs}^l\}$. (In the overlapping case, we need to do the same for the overlapping partition and labeled degree sequences, which we show in Appendix C.)

Choosing prior probabilities is a subtle issue, since it depends on *a priori* assumptions about the data, which usually depends on context, and often requires domain-specific knowledge. In general situations, a prudent approach is to choose uninformative priors, which do not bias the estimation. Here we will take the systematic approach of choosing a nested sequence of priors and hyperpriors, so that an uninformative prior is chosen only at the topmost level [34, 37]. This approach is intended to minimize the sensitivity of the choice of priors, and accordingly provide a shorter description length in the majority of cases.

To generate the partition into groups, we use the process described in detail in Refs. [34, 37], that corresponds to a multilevel Bayesian process, where the distribution of group sizes $\{n_r\}$ (where n_r is the number of nodes in group r) is first uniformly sampled from the set of all allowed possibilities, and the partition is distributed

¹ This may change if the layers are not entirely known, and need to be determined, as in the case with real-valued covariates in Sec. V.

uniformly, conditioned of the observed size distribution, yielding a description length $\mathcal{L}_p = -\ln P(\{b_i\})$ given by

$$\mathcal{L}_p = \ln \left(\binom{B}{N} \right) + \ln N! - \sum_r \ln n_r!, \quad (6)$$

where $\binom{n}{m} = \binom{n+m-1}{m}$ is the total number of m -combinations with repetitions from a set of size n .

For the independent layers model without degree correction, we need to specify the node memberships to each layer. For this, we use the process described in detail in Ref. [37] to generate overlapping partitions. We represent each line in the $\{z_{il}\}$ matrix as a mixture vector \vec{z}_i with C binary entries. We formulate a multilevel Bayesian process, where the distribution of mixture sizes $\{n_d\}$ (where $d_i = \sum_l z_{il}^l$ is the mixture size of node i , and n_d is the number of nodes with $d_i = d$) is generated from all possibilities with uniform probability, and the local values of d_i are sampled from this distribution. The mixture distribution $\{n_{\vec{z}}\}$ (where $n_{\vec{z}}$ is the number of nodes belonging to mixture \vec{z}) is also sampled from the set of possible choices with uniform probability, conditioned of the local mixture sizes $\{d_i\}$, and finally the individual mixtures $\{\vec{z}_i\}$ themselves are sampled from this distribution. This yields a description length $\mathcal{L}_z = -\ln P(\{\vec{z}_i\})$ given by [37]

$$\mathcal{L}_z = \ln \left(\binom{C}{N} \right) + \sum_d \ln \left(\binom{\binom{C}{d}}{n_d} \right) + \ln N! - \sum_{\vec{z}} \ln n_{\vec{z}}!. \quad (7)$$

The *collapsed* degree sequence can be generated with a similar Bayesian process, described also in Ref. [37], that yields a description length $\mathcal{L}_{\kappa} = -\ln P(\{k_i\})$ given by

$$\mathcal{L}_{\kappa} = \sum_r \min \left(\mathcal{L}_r^{(1)}, \mathcal{L}_r^{(2)} \right), \quad (8)$$

with

$$\mathcal{L}_r^{(1)} = \ln \left(\binom{n_r}{e_r} \right), \quad (9)$$

$$\mathcal{L}_r^{(2)} = \ln \Xi_r + \ln n_r! - \sum_k \ln n_k^r!. \quad (10)$$

and $\ln \Xi_r \approx 2\sqrt{\zeta(2)e_r}$.

For layered networks, we need a generative process for the layer-specific degree sequence, $\{k_i^l\}$. Although one could in principle construct nonparametric distributions that incorporate arbitrary correlations among the degree sequences of all layers, the dimension of such distributions is likely to exceed the evidence available in typical data as the number of layers increases. Therefore, here we take the simpler route and assume independent distributions at each layer, so that the description length $\mathcal{L}_{\kappa} = -\ln P(\{k_i^l\})$ becomes simply

$$\mathcal{L}_{\kappa} = \sum_l \mathcal{L}_\kappa(\{k_i\}^l), \quad (11)$$

where $\{k_i\}^l$ should be understood as the collapsed degree sequence of the graph containing only the edges belonging to layer l .

Finally, to generate the edge counts $\{e_{rs}^l\}$, we note that they can be viewed as the adjacency matrix of a layered multigraph with B nodes [59]. Therefore, we may use the stochastic blockmodel itself to generate it, either with independent layers or edge covariates. Since these models have their own edge count parameters, this forms a nested sequence of SBMs, encapsulating the multilevel hierarchical structure of the network, in a fully nonparametric fashion, yielding a description length as described in Ref. [34],

$$\mathcal{L}_e = \sum_{h=1}^L S_m(\{e_{rs}^l\}^h, \{n_r\}^h) + \sum_{h=1}^{L-1} \mathcal{L}_p^h, \quad (12)$$

where $S_m(\{e_{rs}^l\}^h, \{n_r\}^h)$ is the appropriate entropy of the layered SBM in hierarchical level h , and \mathcal{L}_p^h is the description length of the corresponding node partition.

At the top of the hierarchy we have the remaining parameters $\{E_l\}$, denoting the number of edges in each layers. For completeness, they can be easily generated by including an uniform prior $P(\{E_l\}) = \binom{L}{E}^{-1}$, however this only adds an overall constant to the description length, which is not relevant to any comparisons made in this paper.

To summarize, using the shorthand $\{\theta\}$ for the entire set of parameters, we have for each given model (i.e. edge covariates and independent layers, with any optional combination of degree correction and group overlap) an overall description length

$$\Sigma = \mathcal{S}(\{\theta\}) + \sum_{\theta} \mathcal{L}_{\theta}, \quad (13)$$

where $\mathcal{S}(\{\theta\})$ is the appropriate SBM entropy, and \mathcal{L}_{θ} is the description length of a specific parameter ensemble, chosen from Eqs. 6 to 11 (and Eqs. C1 to C2), as appropriate.

B. Confidence levels

As described above, selecting the model with the smallest description length Σ is the appropriate manner of balancing model complexity and goodness of fit. However, often we desire a more refined approach where the alternative model can be accepted or rejected with a degree of confidence, in a nonparametric fashion. This can be achieved, as proposed in Ref. [37], by inspecting the posterior odds ratio [60],

$$\Lambda = \frac{P(\{\theta\}_a | \{G_l\}, \mathcal{H}_a) P(\mathcal{H}_a)}{P(\{\theta\}_b | \{G_l\}, \mathcal{H}_b) P(\mathcal{H}_b)} \quad (14)$$

$$= \exp(-\Delta\Sigma) \frac{P(\mathcal{H}_a)}{P(\mathcal{H}_b)}, \quad (15)$$

where $P(\{\theta\}|\{G_l\}, \mathcal{H})$ is the posterior according to hypothesis \mathcal{H} (i.e. a specific model class), $P(\mathcal{H})$ is any prior belief for hypothesis \mathcal{H} , and $\Delta\Sigma = \Sigma_a - \Sigma_b$ is the difference in description length between both hypotheses. For $\Lambda < 1$ we have that \mathcal{H}_a is rejected over \mathcal{H}_b with a confidence that increases as Λ decreases. Often the values of Λ are divided in subjective intervals of evidence strength [61], as a convention with $\Lambda = 1/100$ being considered the plausibility threshold, below which \mathcal{H}_a is decisively rejected in favor of \mathcal{H}_b , and with $\Lambda \in [1/3, 1]$ being considered only a negligible difference between both models. In the case where there is no preference for either model, $P(\mathcal{H}_a) = P(\mathcal{H}_b)$, the value of Λ is called the Bayes factor [61], which has the same interpretation. In the following, we will always assume $P(\mathcal{H}_a) = P(\mathcal{H}_b)$, and impose $\Lambda \leq 1$, by always putting the preferred hypothesis in the denominator of Eq. 14.

C. Inference algorithm

The description length of a given flavor of the SBM given by Eq. 13 is an objective function that needs to be minimized with some appropriate algorithm. The only known algorithm that is guaranteed to find the global minimum is the exhaustive computation of the description length for every possible hierarchical partition of the network, which is unfeasible in any practical scenario with networks with more than a few nodes and edges. Therefore, we must resort to approximate methods. Here we employ the multilevel MCMC algorithm described in Ref. [62], together with the hierarchical generalization presented in Ref. [34], and the extension to overlapping groups presented in Ref. [37]. The advantage of these algorithms is their good typical running times, and their capacity to overcome metastable states by performing agglomerative moves². The division of the network into layers does not alter these algorithms in any significant way, other than a straightforward book-keeping of the layer membership of each edge. In particular, by using appropriate sparse data structures that do not change in size if the number of layers is increased, the division into layers does not alter significantly the typical running times of the algorithms, which remain $O(N \ln^2 N)$ in their greedy versions, independent of the number of groups B and layers C , and hence are applicable to reasonably large networks. An efficient C++ implementation of these algorithms is freely available as part of the `graph-tool` Python library [65] at <http://graph-tool.skewed.de>.

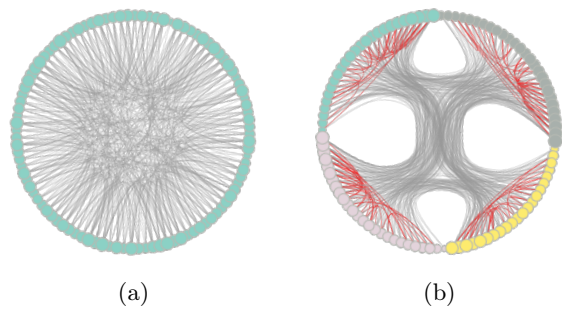


Figure 2. (Color online) Artificial network example containing an informative layered structure. (a) The collapsed graph possesses no discernible structure, i.e. it corresponds to a fully random graph. (b) When the division of edges into two layers [grey and red (light grey)] is taken into account, a four-group structure is revealed.

IV. WHEN ARE LAYERS INFORMATIVE?

Layers are informative of the network structure if their incorporation into the model yields a more detailed description of the data, when compared to a model that is only based on the collapsed structure of the network. An illustration of an informative layered structure is shown in Fig. 2. In this example, an artificial network composed of two layers is constructed. The collapsed graph corresponds to a fully random network, however the division of the edges into layers is such that four fully assortative groups exist in one of the layers. Clearly, the layered division yields structural information that is not discernible in the collapsed graph. This implies that, in more general cases, omitting such information on the edges could potentially significantly obscure structure present in the data [2, 3].

However, it is important to realize that the opposite is also true: If the edge distribution into layers is uncorrelated with the group divisions, it can also obscure structural information which would otherwise be revealed if the layer information were to be ignored. This happens because increasing the number of layers in the model also increases its effective dimension. If the total size and density of the network remains constant as the number of layers increases (and hence the effective dimension of the model), the available data become increasingly sparse, which reduces the inference precision, since it becomes increasingly difficult to distinguish signal from noise. An example of this is shown in Fig. 3, corresponding to a collapsed $B = 2$ assortative SBM with equal-sized groups and edge counts given by $e_{rs} = 2E[\delta_{rs}c/B + (1 - \delta_{rs})(1 - c)/B(B - 1)]$, with $c \in [0, 1]$ being a mixing parameter, where the edges are distributed randomly in C layers. As C increases, both model variants (edge covariates, and independent layers) display increasing degradation when inference is performed, with the detectability transition [66] shifting to higher values of c . For the SBM with independent lay-

² We note that in principle other algorithms such as belief propagation [63] and spectral clustering [64] could be used as well, provided they are suitably adapted to the nonparametric likelihoods considered here.

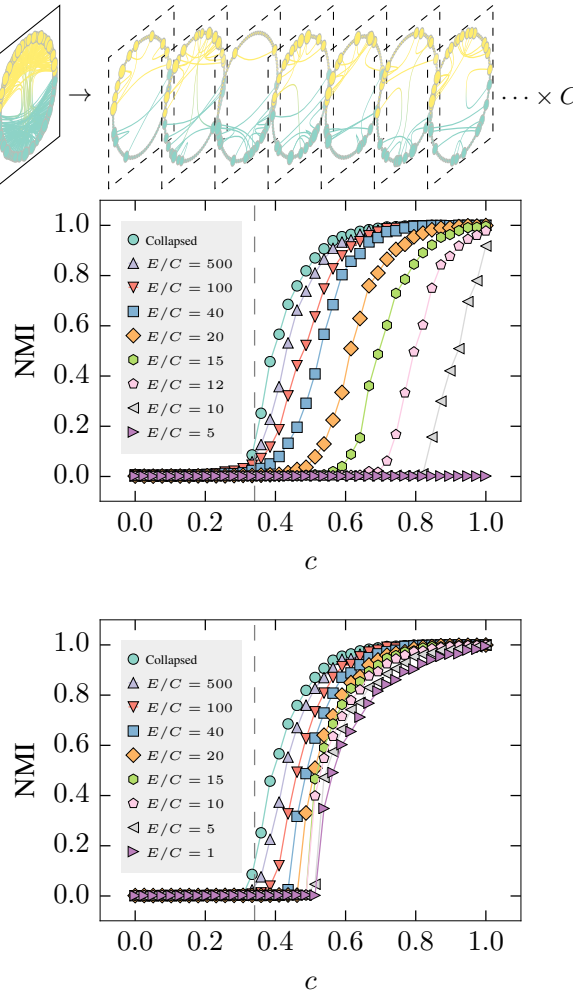


Figure 3. (Color online) An excessive number of layers can obscure network structure. *Top*: A collapsed two-group structure is generated, and the edges are randomly distributed in C layers. *Middle and Bottom*: As the number of edges per layer E/C diminishes, the structure inside each layer becomes increasingly sparse, and the overall quality of the inference worsens. The middle panel shows the normalized mutual information (NMI) between the planted and inferred partitions, using the SBM with independent layers, for a network of $N = 10^4$ nodes and average degree $\langle k \rangle = 2E/N = 14$ as a function of the mixing parameter c , as described in the text. The bottom panel is the same as the middle one, but using the SBM with edge covariates. In both cases the vertical lines mark the detectability transition point for the collapsed SBM, $c^* = 1/B + (B - 1)/(B\sqrt{\langle k \rangle})$ [66].

ers, the transition shifts to $c^* \rightarrow 1$ as $C \rightarrow E$, and in this limit no information at all on the graph structure can be inferred. The version with edge covariates displays a relatively superior performance, with the transition remaining at $c^* < 1$ for $C \rightarrow E$, since it is conditioned on the collapsed graph. Nevertheless, even in this case the degradation caused by increasing C is very noticeable.

Because of this problem, it is important to consider if we indeed need the layered structure to describe the

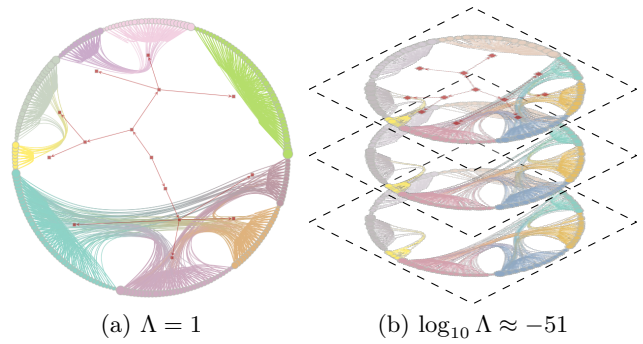


Figure 4. (Color online) Two generative models for a layered social network of physicians [67]. (a) Inferred DCSBM for the collapsed network, with the edges assumed to be randomly distributed among the layers. (b) Inferred DCSBM with edge covariates, where each layer corresponds to one type of acquaintance. Below each figure is shown the posterior odds ratio Λ , relative to preferred model (a). The circular layout with edge bundling [68] represents the inferred node hierarchy (indicated also by the red nodes and edges), as explained in the text (see also Ref. [34]).

large-scale structure of a network, or if it needs to be coarse-grained or even discarded. This can be done by considering a null model where the edges are distributed among the layers in a manner that is entirely independent of the group structure, and is parametrized only by the total number of edges in each layer, $\{E_l\}$. Let us use the shorthand $\{\theta\}$ for the possible set of parameters of a collapsed SBM. This null model has a likelihood given simply by

$$P(\{G_l\}|\{\theta\}, \{E_l\}) = P(G_c|\{\theta\}) \times \frac{\prod_l E_l!}{E!} \quad (16)$$

where the first term is the likelihood of the collapsed SBM and the second accounts for the random distribution of edges across the layers (the above equation is valid only for simple graphs; for multigraphs see Appendix A). The full posterior and its corresponding description length are computed just as before, by including the priors for $\{e_{rs}\}$, $\{b_i\}$, $\{\vec{b}\}$, $\{k_i\}$ and $\{\vec{k}_i\}$. We can then compare the description length of this null model with any of the other layered variants, and decide if there is enough evidence to justify the incorporation of layers that are correlated with the group structure.

As a concrete example, here we consider an empirical social network of $N = 241$ physicians, collected during a survey [67]. Participants were asked which other physicians they would contact in hypothetical situations. The questions asked were: 1. “When you need information or advice about questions of therapy where do you usually turn?”, 2. “And who are the three or four physicians with whom you most often find yourself discussing cases or therapy in the course of an ordinary week – last week for instance?”, 3. “Would you tell me the first names of your three friends whom you see most often socially?”. The answers to each question represent edges in one specific

layer of a directed network. If one applies the DCSBM to the collapsed graph (which provides the best fit among the alternatives), it yields a division into $B = 9$ groups, as shown in the left panel of Fig. 4, including also a division into three disconnected components (corresponding to different cities). Between the layered SBM versions, the model with edge covariates that turns out to be a better fit to the data (i.e. yields a lower description length) and divides the network into $B = 8$ groups, as shown in the left panel of Fig. 4. When inspecting the edge counts visually, one does not notice any significant difference between the patterns in each layer. Indeed, when comparing the description lengths between the null model with random layers above and the SBM with edge covariates, we find that the latter is strongly rejected with a posterior odds ratio $\Lambda \approx 10^{-51}$. Therefore, there is no noticeable evidence in the data to support any correlation of layer divisions with the large-scale structure present in the graph. This suggests that the important descriptors of this social network are mainly the overall acquaintances among physicians, not their precise types (at least as measured by the survey questions).

We now turn to another example, where informative layered structure can be detected. We consider the vote correlation network of federal deputies in the Brazilian national congress. Based on public data containing the votes of all deputies in all chamber sessions across many years³, we obtained the correlation matrix between all deputies. We constructed a network by connecting an edge from a deputy to other 10 deputies with which she is most correlated in the considered period⁴. We then separated the network in two layers, corresponding to two consecutive four-year terms, 1999 – 2002 and 2003 – 2006. Deputies not present during the whole period were removed from the network, yielding a network with $N = 224$ nodes and $E = 7247$ edges in total. When fitting the DCSBM for the collapsed network (which is again the best model), we obtain the $B = 11$ partition shown in the left panel of Fig. 5. It shows a hierarchical division that is largely consistent with party and coalition lines, as well as positions in the political spectrum (with a noticeable deviation being a group of left-wing parties composed by PDT, PSB and PCdoB being grouped together with center-right parties PTB and PMDB). When incorporating the layers, the best model fit is obtained by the DCSBM with independent layers, which yields a $B = 11$ division mostly compatible with (but not fully identical to) the collapsed network, although with a different hierarchical structure, as can be seen in the right panel of Fig. 5. However, the layered representation of this network reveals a major coalition change between the two terms, consistent with the shift of power that occurred with the election of a new president belonging to

the previous main opposition party: In the 1999 – 2002 term we see a clear division into a government and opposition groups (as captured in the topmost level of the hierarchy), with most edges existing between groups of the same camp, corresponding to a right-wing/center government led by the PSDB, PMDB, PFL, DEM and PP parties, and a left-wing opposition composed mostly by PT, PDT, PSB and PCdoB. After 2002, we observe a shifted coalition landscape, with a left-wing/center government predominantly formed by PT, PMDB, PDT, PSB and PCdoB, and an opposition led by PSDB, PFL, DEM and PP. Because of this noticeable change in the large-scale network structure — that is completely erased in the collapsed network — the null model with random layers ends up being forcefully rejected with $\Lambda \approx 10^{-111}$, meaning that the layered structure is very informative on the network structure.

In the above examples we made a comparison between the layered model and a null model with fully random layers. In some scenarios we might be interested in a more nuanced approach, where the layers are coarse-grained with a more appropriate level of granularity. This can be done by merging some of the layers into bins, such that inside each bin the layer membership of the edges is distributed regardless of the group structure. Let ℓ specify a set of layers that were merged in one specific bin, and $\{\theta\}_{\{\ell\}}$ be a shorthand for the possible set of parameters of a layered SBM $\{G_\ell\}$ (with independent layers or edge covariates) where each bin ℓ corresponds to an individual layer. The likelihood of this model conditioned on a specific bin set $\{\ell\}$ is given by

$$P(\{G_l\} | \{\theta\}_{\{\ell\}}, \{\ell\}) = P(\{G_\ell\} | \{\theta\}_{\{\ell\}}) \times \prod_{\ell} \frac{\prod_{l \in \ell} E_l!}{E_\ell!}, \quad (17)$$

where $E_\ell = \sum_{l \in \ell} E_l$ is the number of edges in bin ℓ (the above equation is valid only for simple graphs; See Appendix A for the more general case with parallel edges). When considering the full posterior, we need to include the priors for $\{\theta\}_{\{\ell\}}$ as before, but also for the binning $\{\ell\}$ itself. If the layers can be grouped arbitrarily, we have

$$P(\{\ell\}) = \frac{\prod_\ell n_\ell!}{C!} \times \left(\binom{M}{C} \right)^{-1} \quad (18)$$

where n_ℓ is the number of layers in bin ℓ and M is the total number of layer bins. If the layers are inherently ordered, and thus can only be contiguously binned, this becomes instead simply

$$P(\{\ell\}) = \left(\binom{M}{C} \right)^{-1}. \quad (19)$$

If we make $M = 1$ we recover the original null model above. Algorithmically, one can find the appropriate bins in a variety of ways. A simple approach is to use agglomerative hierarchical clustering, i.e. by putting at first each

³ Available at <http://www.camara.gov.br/>.

⁴ We experimented with other threshold values, and obtained similar results.

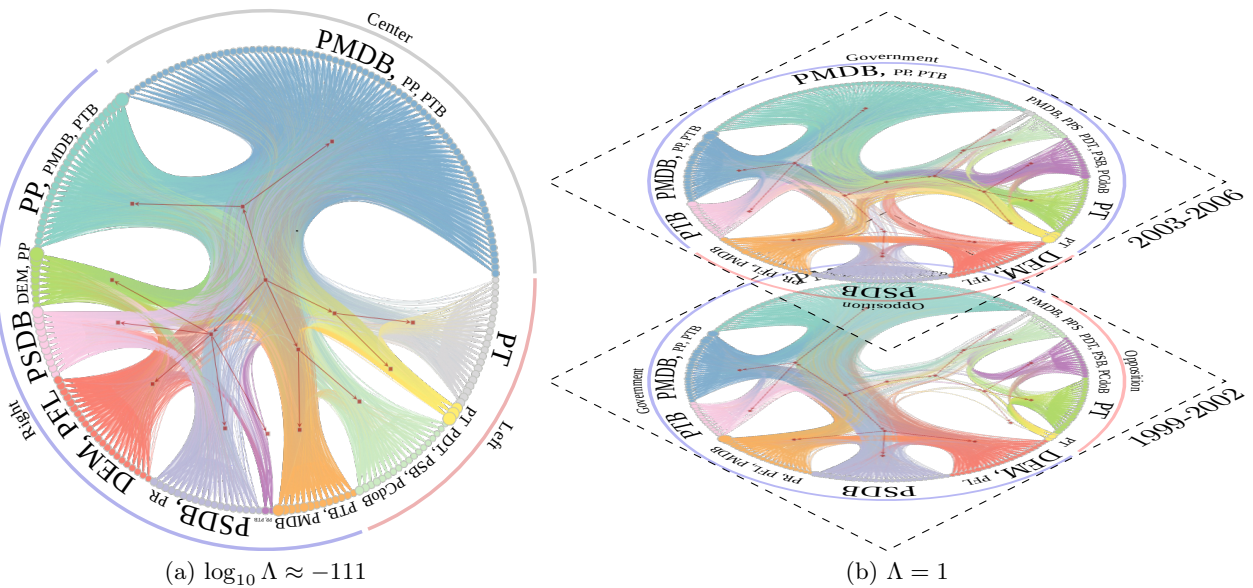


Figure 5. (Color online) Network of vote correlations among federal deputies of the Brazilian national congress during two consecutive four-year terms, 1999 – 2002 and 2003 – 2006. (a) DCSBM fit for the collapsed network obtained by merging both terms, corresponding to a null model where the edges are randomly distributed between the layers. The group labels correspond to the predominant parties inside each group, determined after the inference had been performed (the size of the label indicates the proportion of each party inside the group). (b) DCSBM with independent layers for the network divided into two terms. In both cases is shown the posterior odds ratio Λ relative to the best model [in this case (b)]. The layout is the same as in Fig. 4.

layer in its own bin, and subsequently merging bins according to the reduction of the overall description length. We explore this idea further in Sec V, when dealing with real-valued edge covariates.

A. Layers as evidence for overlaps

There is an important correspondence between layered networks and overlapping structures of collapsed networks. Namely, the inference of overlapping structures in collapsed graphs can to some extent be interpreted as the inference of latent layers [40] to which the edges belong, where each (connected) group pair (r, s) would correspond to a different layer. Because of this correspondence, any a priori knowledge of the division into layers can fundamentally alter the interpretation of the data in situations where a nonoverlapping model would otherwise be considered a better fit for the collapsed network [37].

This is better understood by considering the following generative process as an example: A network is generated with C layers, where in each layer E/C edges are randomly placed between the nodes that belong to that layer. The layer membership mixtures are parameterized as $n_{\vec{z}} \propto \prod_l \mu^{z_l}$, up to a normalization constant, and with $\mu \in [0, 1]$ controlling the degree of layer overlap: For $\mu \rightarrow 0$ we obtain asymptotically nonoverlapping layers with $n_l = N/B$ nodes at each layer l , and for $\mu = 1$ all mixtures \vec{z} have the same size. This process corresponds

to a layered SBM with only one group, $B = 1$, and the aforementioned layer structure. If we consider only the collapsed graph, with the layer information removed, the corresponding topology can be generated in two alternative ways: 1. An overlapping SBM with $B = C$ groups and mixtures $\vec{b}_i = \vec{z}_i$, and edge counts $e_{rs} = 2E\delta rs/B$. 2. A nonoverlapping SBM with each individual mixture as its own group, indexed by $r_{\vec{b}} = \sum_{s=1}^B b_s 2^{s-1} \in [1, 2^C - 1]$, resulting in a total of $B = 2^C - 1$ groups, and edge counts given by

$$e_{r_{\vec{b}_1} r_{\vec{b}_2}} = \sum_{rs} b_1^r b_2^s \frac{e_{rs}}{n_r n_s} n_{r_{\vec{b}_1}} n_{r_{\vec{b}_2}}. \quad (20)$$

The description length of the *collapsed graph* generated with the layered model is

$$\Sigma_c = 2E - E \ln \frac{2EC}{N^2} + \mathcal{L}_z(\{n_{\vec{z}}(\mu)\}), \quad (21)$$

which is in fact identical to the overlapping SBM, corresponding to $C \rightarrow B$ and $n_{\vec{z}}(\mu) \rightarrow n_{\vec{b}}(\mu)$ in the above equation. The nonoverlapping model, on the other hand, has a description length given by

$$\Sigma'_c = 2E - \frac{1}{2} \sum_{\vec{b}_1 \vec{b}_2} e_{r_{\vec{b}_1} r_{\vec{b}_2}} \ln \frac{e_{r_{\vec{b}_1} r_{\vec{b}_2}}}{n_{r_{\vec{b}_1}} n_{r_{\vec{b}_2}}} + \mathcal{L}_p(\{n_{r_{\vec{b}}}(\mu)\}), \quad (22)$$

where $\mathcal{L}_p(\{n_{r_{\vec{b}}}(\mu)\})$ corresponds to a nonoverlapping partition of individual mixtures. As discussed in Ref. [37], we may have $\Sigma'_c < \Sigma_c$ if the number of nodes at the

intersections is sufficiently large. Therefore the nonoverlapping model may indeed be considered the most parsimonious of the three in that case, which is arguably non-intuitive, since the overlapping SBM seems closer to the original model. However, the situation changes when the observed data includes the layer information on the edges. In this case, we must include the random division of the edges into layers in the two collapsed models, by adding, according to Eq. 16, the following term to the description length:

$$\ln E! - \sum_l \ln E_l! = \ln E! - C \ln E/C!. \quad (23)$$

Because of this difference, the layered model with $B = 1$ becomes always the preferred choice (see Fig. 6). Therefore, when edge information is available, it can significantly change which model is preferred, and tip the scale towards the overlapping description. However, we emphasize that this extra information does nothing regarding the decision between both collapsed models; it only supports the acceptance of the third layered variant.

It is important to consider the above comparison together with the results of Ref. [37], which showed that the overlapping variants of the SBM are seldom the best fit for the majority of empirical networks used for that work, which contained no layer information. As the example above shows, this assessment may change (at least in principle) if any division among the edges can be assumed *a priori*. Therefore, for a fair assessment of the best generative process, it is imperative to leverage all available information, in particular the division into layers, or the existence of edge covariates.

V. EDGES WITH REAL-VALUED CORRELATES

The models discussed so far are capable of generating data with discrete values associated with the existing edges. However, in many important situations the values associated with edges are real values, corresponding to weights, distances, capacities, etc. Here we show how the previous models can be straightforwardly adapted to these cases as well, using a discretization approach. As before, we simply assume that the graph is divided into C discrete layers, however we ascribe to each layer l a real value x_l , randomly sampled from a PDF $\rho(x)$, such that all edges in the same layer possess the same edge correlate. In the case that all edges have a different correlate, we will have $C = E$ layers. Like in Sec. IV we assume that the layers themselves are grouped into bins $\{\ell\}$, with $\{\theta\}_{\{\ell\}}$ being a shorthand for the possible set of parameters of a layered SBM (with independent layers or edge covariates) $\{G_\ell\}$ where each bin ℓ corresponds to an individual layer. The whole PDF of the data generated

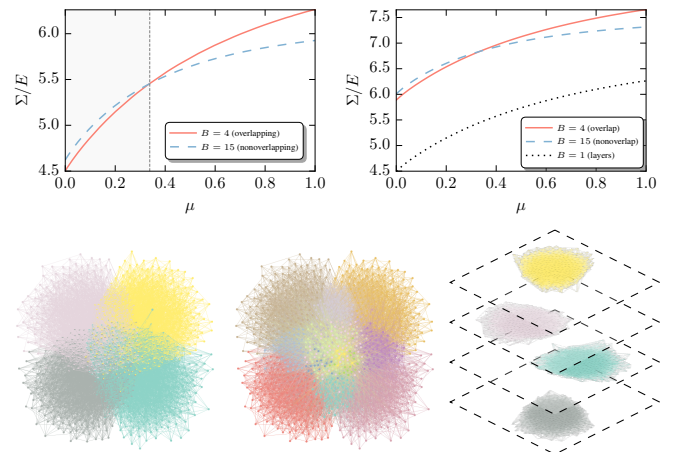


Figure 6. (Color online) *Top left*: Description length per edge Σ/E for the collapsed planted partition model described in the text as a function of the overlap parameter μ , with $N = 10^3$, $\langle k \rangle = 2E/N = 10$ and $B = 4$ (illustrated in the lower left panel). The two curves show the description length of the planted overlapping model, and the equivalent non-overlapping model with $2^B - 1$ groups (illustrated in the lower middle panel). Only for values of μ below the intersection point the original overlapping model is preferred over the nonoverlapping one. *Top right*: The same as in the top left, but with layer information included. The third curve corresponds to a $B = 1$ model with $C = 4$ independent layers (illustrated in the lower right panel), whereas the first two curves correspond to the same collapsed models as in the left panel, but with a random distribution of edges in the $C = 4$ layers. The model with independent layers is preferred over the alternatives in the entire parameter range.

in this manner becomes

$$P(\{G_x\}|\{\theta\}_{\{\ell\}}, \{\ell\}) = P(\{G_\ell\}|\{\theta\}_{\{\ell\}}, \{\ell\}) \times \prod_l \rho(x_l), \quad (24)$$

where the first term is given by Eq. 17. The advantage of this approach is that the overall correlate PDF $\rho(x_l)$ amounts to constant multiplicative factor in the likelihood, independent of our choice of bins, and therefore cannot influence either the maximum likelihood estimate or the maximum of the posterior distribution, and therefore for these purposes we can avoid specifying it altogether. This contrasts with another generalization of the SBM for real-valued covariates proposed in Ref. [49], which requires the exact form of the correlate distribution to be specified prior to inference (on the other hand, the approach presented here is based the discretization of the correlates into bins, whereas in Ref. [49] no binning is necessary).

In order to choose the best number of layers, we maximize the posterior $P(\theta_{\{\ell\}}, \{\ell\} | \{G_x\})$, which involves the priors of the SBM parameters, as well as for the bins $\{\ell\}$, as given by Eq. 19. Therefore, both the number and the boundary positions of the bins can be determined in a nonparametric manner, based only on the data.

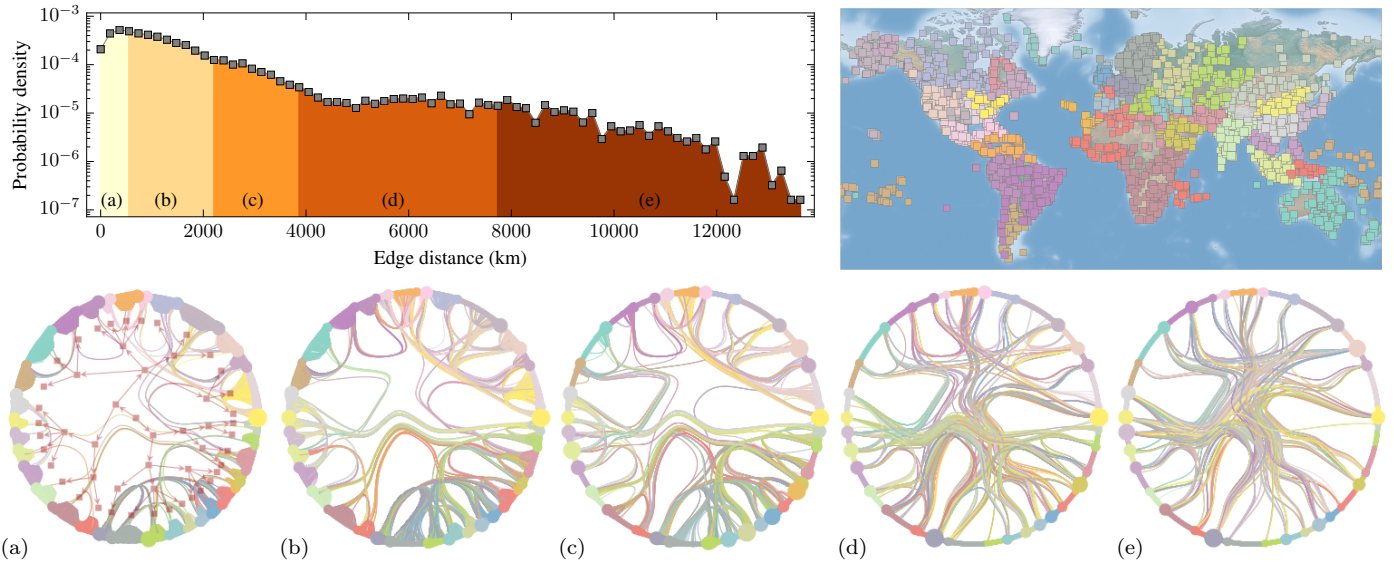


Figure 7. (Color online) Global airport network of openflights.org. *Top left:* Distribution of edge distances. The bins labeled from (a) to (e) correspond to the best division of the edges into layers according to the method described in the text. *Top right:* Spatial distribution of airports. The colors correspond to the division of the network into groups, according to the best fit of the DCSBM model with independent layers (the same color coding is used in the remaining panels). *Bottom:* Individual layers of the DCSBM fit, corresponding to the bins in the top panel. The layout is the same as in Fig. 4.

As an example we consider the global airport network as collected by openflights.org. This is a directed multigraph, where the $N = 3253$ nodes are airports and the $E = 67154$ edges represent existing flights. Since the position of the airports is known, we can characterize the edges by their geodesic distance, which we treat as a covariate. In applying the DCSBM with independent layers, using the method outlined above to find the optimal binning of the distances, we find a division into $B = 34$ groups, and $M = 5$ distance bins, as shown in Fig. 7. When inspecting the spatial distribution of airports, we observe that the obtained groups correspond to fairly contiguous geographical regions (see Fig. 7, top right). The distribution of edges across the layers reveal a hierarchical organization strongly correlated with flight distance: The first layer captures local “intra-groups” with relatively short distance, whereas the upper layers capture increasingly “inter-groups” flights with longer distances. The nodes with large degree tend to be those that belong to multiple layers, i.e. major airport hubs that service both short and long-distance flights.

can use the same approach as in the previous section⁵. By using the different model versions presented in this work, different types of temporal patterns can be captured. In all cases, by separating the network into time-bins, it is assumed that inside each bin the edges are placed between the groups in a random fashion, conditioned only on the group membership of the receiving nodes. When using the SBM with edge covariates, the nodes are assumed to belong to all time layers, and as such can receive edges at all times, depending only on the activity of the entire group at any give time. On the other hand, the version with independent layers allows for a individualized placement of the nodes into the layers (independently of their group membership) such that their activity may be separately regulated. The activity inside each layer can be even more fine-tuned in the degree-corrected model with independent layers, since the degree of each node at each time window is separately specified. In all these examples, the group memberships are forced to be stable in time. This can be changed by using an overlapping SBM [37], where the group memberships (which are in this case attributes of the *half-edges* of the graphs) can change arbitrarily in time. As before, given some empirical observation, the most appropriate model choice is the one with the minimum description length.

The discretization approach presented here is similar in

VI. TIME-VARYING NETWORKS

Temporal networks can be viewed as a special case of networks with real-valued edge correlates representing their existence at a specific time, $x_i = t_i$, and hence we

⁵ Other formulations of temporal networks are possible. For instance, one could attribute to each edge a tuple $\vec{x}_i = (t_i^b, t_i^e)$, containing a creation and deletion time, respectively. The approach presented here can be adapted to such a multivariate case in a straightforward manner, by using multidimensional bins.

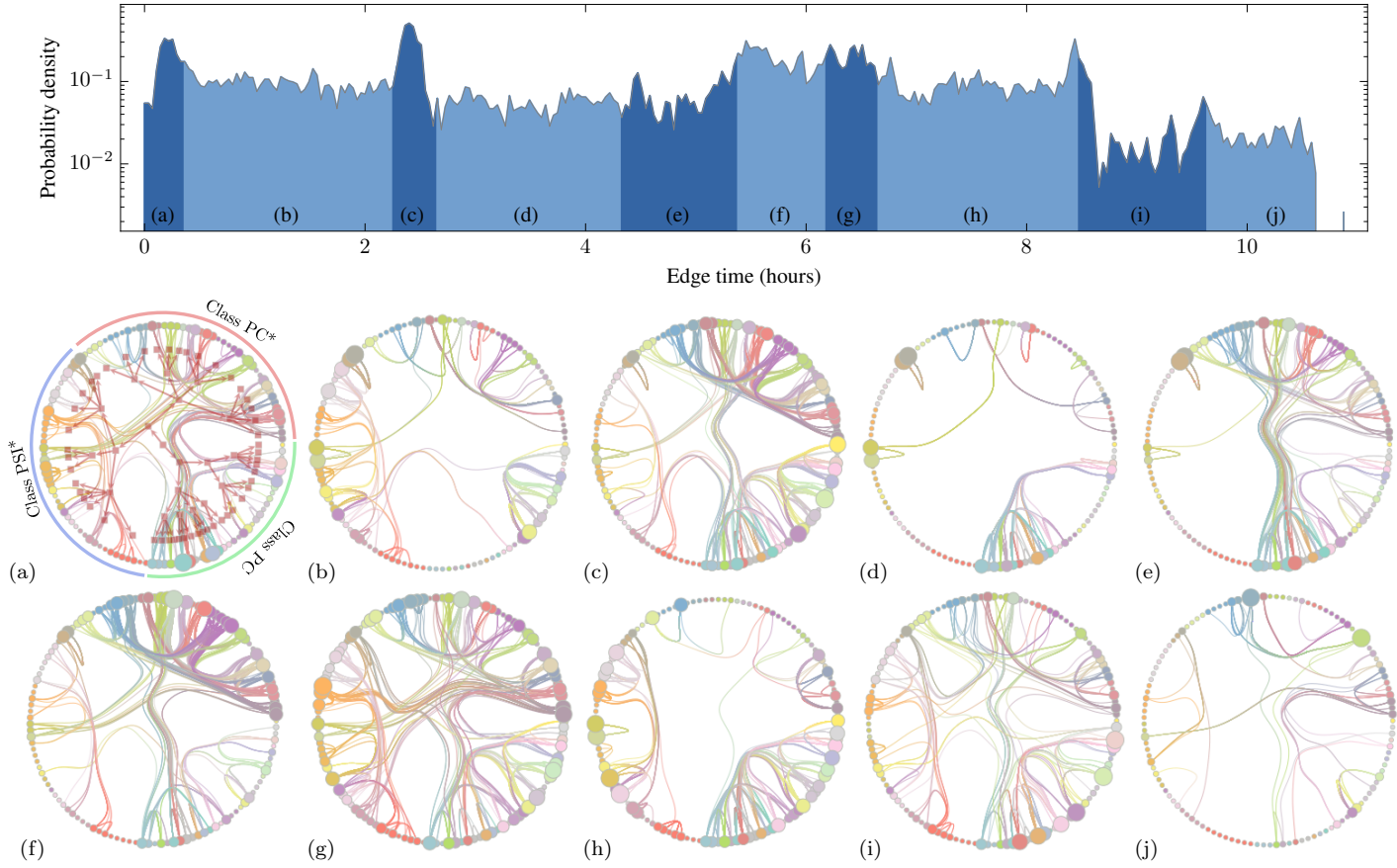


Figure 8. (Color online) Proximity network between high-school students [69]^a. *Top*: Network activity (i.e. probability density of an edge being present) as a function of time, over a period of one day. The bins labeled from (a) to (j) correspond to the best division of the edges into layers according to the method described in the text. *Bottom*: Individual layers of the DCSBM fit, corresponding to the bins in the top panel. The layout is the same as in Fig. 4.

^a Retrieved from <http://sociopatterns.org>.

spirit to the detection of “change points” in networks [39]. Since it is assumed that inside each time window the edges are placed in a manner that is independent of their time relative to one another, the most appropriate time binning is the one that partitions the time series in such a way that inside each time window the large-scale network structure does not change significantly. The interface between two bins can therefore be interpreted as change points where the large-scale structure has changed in a measurable and statistically significant way.

Here we show an application of this method to a time-resolved proximity network between $N = 126$ high-school students, recorded over a period of four days in 2011 [69], of which we isolated only the first day to simplify the analysis. In this experiment, volunteering students wore proximity sensors during school hours, which recorded an edge and its time if two students were below a distance threshold for a pre-specified amount of time. If we apply the DCSBM with independent layers to this dataset (again providing a better fit), the best partition is found for $B = 33$ groups, and the whole time series was divided into $M = 10$ periods, as can be seen in Fig. 8.

The hierarchical partition is in accordance with the existence of three classes, as can be seen in the first levels of the hierarchy. Each period marks a region in time where a distinct large-scale structure is observed. These periods alternate between those with high activities and those with a relative quiescence, presumably representing breaks (with many edges between classes, and a perceived synchrony between the PC and PC* classes) and class periods (with few edges between classes), respectively, although this information is not available in the dataset.

In the above example, the best fit was obtained for a nonoverlapping SBM, implying that the group memberships remain stable in time. However, in some situations, movements between groups can be inferred. As an example, we return to the network of vote correlations of the Brazilian national congress. Differently from before, now we inspect a single four-year term from 2007 to 2010, and we separate each year into one layer, yielding a network with $N = 475$ nodes and $E = 9053$ edges in total. In this case, a best fit is obtained for an *overlapping* DCSBM with independent layers and $B = 12$ groups, as seen in

Fig. 9. The hierarchical division clearly separates between a center-left government coalition (the largest topmost branch) and the right-wing opposition (the smallest topmost branch). In the government branch, we observe the existence of many “peripheral” deputies, which are not strongly correlated with each other, and instead are aligned with smaller groups of more connected nodes, which are divided mostly along party lines. This property is weakened in the later years of the term, as more edges are observed between peripheral deputies. The overlapping structure found is correlated strongly with the layered divisions, such that by observing only one layer in isolation, no overlaps are present. Therefore, a fraction of the deputies seem to completely change their alignment patterns in successive years, as shown in the bottom of Fig. 9. The flow between groups is mostly confined to either the government or opposition groups, with the majority of the activity occurring inside the government faction. Although some deputies did change their party affiliation during this period, the observed flows seem mostly uncorrelated with this, and instead appears to show a more fine-grained alignment between deputies that is not uniquely defined by their party membership.

VII. CONCLUSION

We presented a framework for the nonparametric inference of mesoscale structures in layered, edge-valued and time-varying networks, based on a variety of modifications of the stochastic block model, incorporating features such as hierarchical structure, degree-correction, and overlapping groups. These models were formulated in a Bayesian setting, that allows the identification of the most appropriate model variant based on statistical evidence, corresponding to a principled balance between model complexity and quality of fit.

We have identified an important pitfall when analyzing network data with layered structure, where the inclusion of many layers that are uncorrelated with the mesoscale structure can obstruct its identification. This problem cannot be neglected if the number of layers becomes large, as in the case of temporal or edge-value networks where the layers correspond to arbitrary bins of the edge covariates. We expect this problem to affect also non-statistical methods based on modified modularity maximization [4, 20, 21, 26, 28], as well as flow compression [22] and non-negative tensor factorization [27]. In our setting, we have shown how this can be completely avoided by comparing the inferred model with a null model that assumes that the layers are uncorrelated, or with a coarse-grained version that condenses uncorrelated layers into bins.

We also showed how this framework can be extended in a straightforward manner to networks with real-valued attributes on the edges, and temporal networks. The proposed methodology is capable of identifying specific scales — both of the edge values and in time — where

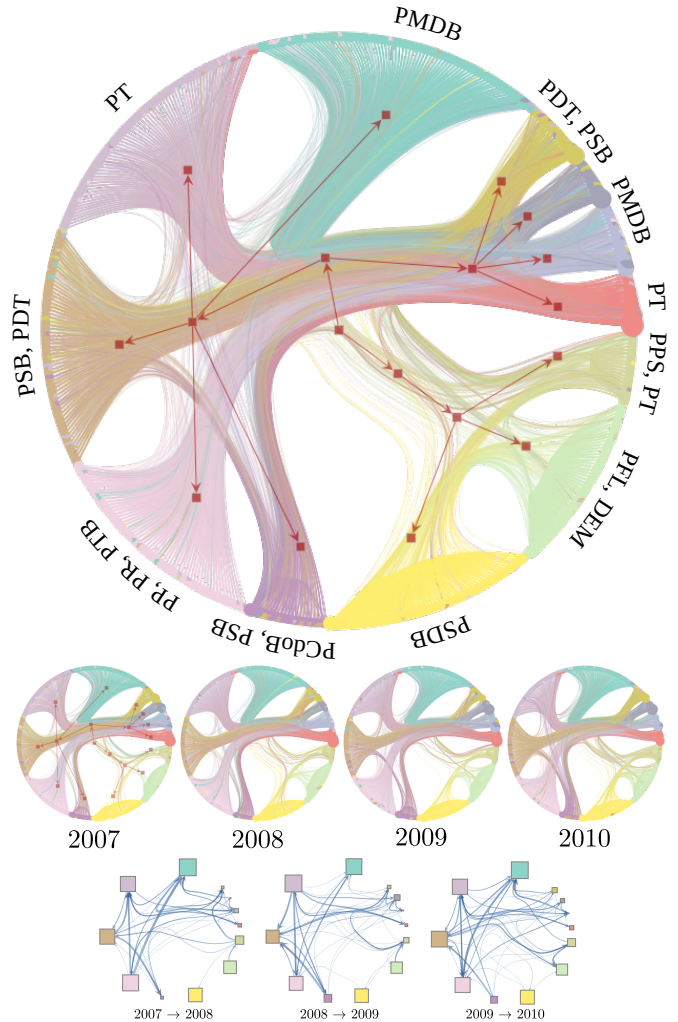


Figure 9. (Color online) Network of vote correlations among federal deputies of the Brazilian national congress in the four-year term from 2007 to 2010. The top panel shows the $B = 12$ division obtained by fitting an overlapping DCSBM with independent layers, with all layers collapsed into one figure. The group labels correspond to the predominant parties inside each group. The individual layers can be seen in the middle panel. The bottom panel shows the flows of deputies between each group after each year. The edge thickness corresponds to the amount of deputies, with the largest flow corresponding to 10 deputies, and the smallest 1 deputy.

the mesoscale structure does not change significantly, enabling the identification of the most appropriate coarse-graining of the network in discrete layers, as well as the detection of “change points” of the network structure.

The unsupervised inference of the most parsimonious layered model, as well as the appropriate granularity of the layers, based solely on statistical evidence and requiring no *ad hoc* parameters, provides a principled and robust method to analyze multilayer, temporal and edge-valued network data. This approach is likely to be directly useful in a variety of tasks, such as the nonparametric modeling of correlation networks [21], the pre-

dition of missing valued edges [47, 48], the identification of relevant time scales in temporal networks [70], and its relation to dynamical processes taking place on them [71, 72], among many others.

ACKNOWLEDGMENTS

I would like to thank Ricardo Marino for compiling and kindly providing the voting data of the chamber of deputies in the Brazilian national congress, Roger Guimerà and Marta Sales-Pardo for insightful discussions, as well as Mason Porter and Martin Rosvall for helpful comments on the manuscript. This work was funded by the University of Bremen, under the program ZF04.

Appendix A: Multigraphs

For multigraphs, we need to consider that parallel edges that belong to the same layer are indistinguishable. Hence the likelihoods of Eq. 2 must be corrected to read

$$P(\{G_l\}|\{\theta\}) = P(G_c|\{\theta\}) \prod_{r \leq s} \frac{\prod_l m_{rs}^l!}{m_{rs}!} \times \frac{\prod_{i>j} A_{ij}!}{\prod_{i>j,l} A_{ij}^l!} \frac{\prod_i A_{ii}/2!}{\prod_{i,l} A_{ii}^l/2!}. \quad (\text{A1})$$

The last term does not depend on the SBM parameters. Therefore, when doing inference, the difference amounts to multiplicative constant which does not alter the position of the most likely network partition, and thus could in principle be discarded. However, this difference is important when comparing models with a different number of layers, as will be done below.

For the independent layers model, it suffices to use the appropriate multigraph likelihood in each layer, as is given in Refs. [37, 55].

Likewise, when considering the null model of Sec. IV, the existence of parallel edges must also be accounted for. Therefore Eq. 16 must be modified to read

$$P(\{G_l\}|\{\theta\}, \{E_l\}) = P(G_c|\theta) \times \frac{\prod_l E_l!}{E!} \times \frac{\prod_{i>j} A_{ij}!}{\prod_{i>j,l} A_{ij}^l!} \times \frac{\prod_i A_{ii}/2!}{\prod_{i,l} A_{ii}^l/2!}. \quad (\text{A2})$$

In the case of binned layers, it must be analogously modified to read

$$P(\{G_l\}|\theta_{\{\ell\}}, \{\ell\}) = P(\{G_\ell\}|\theta_{\{\ell\}}) \times \prod_\ell \frac{\prod_{l \in \ell} E_l!}{E_\ell!} \times \prod_{i>j} \prod_\ell \frac{A_{ij}^\ell!}{\prod_{l \in \ell} A_{ij}^l!} \times \prod_i \prod_\ell \frac{A_{ii}^\ell/2!}{\prod_{l \in \ell} A_{ii}^l/2!}. \quad (\text{A3})$$

Appendix B: Directed graphs

Directed graphs represent straightforward modifications of the models presented in the main text. For the collapsed likelihoods and priors, we refer the Refs. [37, 55].

For the model with edge covariates and the possibility of multiple edges, the total likelihood of Eq. 2 becomes simply

$$P(\{G_l\}|\{\theta\}) = P(G_c|\{\theta\}) \prod_{rs} \frac{\prod_l m_{rs}^l!}{m_{rs}!} \times \frac{\prod_{ij} A_{ij}!}{\prod_{ij,l} A_{ij}^l!}. \quad (\text{B1})$$

And again, for the independent layers model, it suffices to use the appropriate directed likelihood in each layer, as is given in Refs. [37, 55].

Likewise, when considering the null model of Sec. IV, for directed graphs (with possible multiple edges) Eq. 16 must be modified to read

$$P(\{G_l\}|\{\theta\}, \{E_l\}) = P(G_c|\theta) \times \frac{\prod_l E_l!}{E!} \times \frac{\prod_{ij} A_{ij}!}{\prod_{ij,l} A_{ij}^l!}, \quad (\text{B2})$$

and in the case of binned layers,

$$P(\{G_l\}|\theta_{\{\ell\}}, \{\ell\}) = P(\{G_\ell\}|\theta_{\{\ell\}}) \times \prod_\ell \frac{\prod_{l \in \ell} E_l!}{E_\ell!} \times \prod_{ij} \prod_\ell \frac{A_{ij}^\ell!}{\prod_{l \in \ell} A_{ij}^l!}. \quad (\text{B3})$$

Appendix C: Model selection for overlapping groups

In the case the SBM with overlapping groups, we need to specify a generative process for the overlapping partition into B groups $\{\vec{b}_i\}$, and the collapsed (or layer-specific) labeled degree-sequence $\{\vec{k}_i\}$ (or $\{\vec{k}_i^l\}$).

To generate the overlapping partition into groups, we use the hierarchical process described in detail in Ref. [37], already described in the main text adapted to the generation of the layer-membership matrix $\{z_{il}\}$, which yields $\mathcal{L}_p = -\ln P(\{\vec{b}_i\})$ given by

$$\mathcal{L}_p = \ln \left(\binom{D}{N} \right) + \sum_d \ln \left(\binom{B}{n_d} \right) + \ln N! - \sum_{\vec{b}} \ln n_{\vec{b}}!, \quad (\text{C1})$$

where $D \leq B$ is the maximum mixture size d . The case without group overlaps amounts to $D = 1$, reducing it to Eq. 6.

The *collapsed* overlapping degree sequence can be generated with a similar Bayesian process, described also

in Ref. [37], that yields a description length $\mathcal{L}_\kappa = -\ln P(\{\vec{k}_i\})$ given by

$$\mathcal{L}_\kappa = \sum_r \ln \left(\binom{m_r}{e_r} \right) + \sum_{\vec{b}} \min \left(\mathcal{L}_{\vec{b}}^{(1)}, \mathcal{L}_{\vec{b}}^{(2)} \right). \quad (\text{C2})$$

with

$$\mathcal{L}_{\vec{b}}^{(1)} = \sum_r \ln \left(\binom{n_{\vec{b}}}{e_{\vec{b}}^r} \right), \quad (\text{C3})$$

$$\mathcal{L}_{\vec{b}}^{(2)} = \sum_{r \in \vec{b}} \ln \Xi_{\vec{b}}^r + \ln n_{\vec{b}}! - \sum_{\vec{k}} \ln n_{\vec{k}}!. \quad (\text{C4})$$

where $\ln \Xi_{\vec{b}}^r \approx 2\sqrt{\zeta(2)e_{\vec{b}}^r}$. For the case without overlaps this reduces to Eq. 8. The edge-specific overlapping degree sequence is obtained according to Eq. 11.

-
- [1] Mark Newman, *Networks: An Introduction* (Oxford University Press, 2010).
- [2] Mikko Kivelä, Alex Arenas, Marc Barthelemy, James P. Gleeson, Yamir Moreno, and Mason A. Porter, “Multilayer networks,” *jcomplexnetw* **2**, 203–271 (2014).
- [3] S. Boccaletti, G. Bianconi, R. Criado, C. I. del Genio, J. Gómez-Gardeñes, M. Romance, I. Sendiña-Nadal, Z. Wang, and M. Zanin, “The structure and dynamics of multilayer networks,” *Physics Reports The structure and dynamics of multilayer networks*, **544**, 1–122 (2014).
- [4] Manlio De Domenico, Albert Solé-Ribalta, Emanuele Cozzo, Mikko Kivelä, Yamir Moreno, Mason A. Porter, Sergio Gómez, and Alex Arenas, “Mathematical Formulation of Multilayer Networks,” *Phys. Rev. X* **3**, 041022 (2013).
- [5] Petter Holme and Jari Saramäki, “Temporal networks,” *Physics Reports* **519**, 97–125 (2012).
- [6] Sergey V. Buldyrev, Roni Parshani, Gerald Paul, H. Eugene Stanley, and Shlomo Havlin, “Catastrophic cascade of failures in interdependent networks,” *Nature* **464**, 1025–1028 (2010).
- [7] M. Dickison, S. Havlin, and H. E Stanley, “Epidemics on Interconnected Networks,” arXiv:1201.6339 (2012).
- [8] Li Chen, Fakhteh Ghanbarnejad, Weiran Cai, and Peter Grassberger, “Outbreaks of coinfections: The critical role of cooperativity,” *EPL* **104**, 50001 (2013).
- [9] Eugenio Valdano, Luca Ferreri, Chiara Poletto, and Vittoria Colizza, “Analytical Computation of the Epidemic Threshold on Temporal Networks,” *Phys. Rev. X* **5**, 021005 (2015).
- [10] S. Gómez, A. Díaz-Guilera, J. Gómez-Gardeñes, C. J. Pérez-Vicente, Y. Moreno, and A. Arenas, “Diffusion Dynamics on Multiplex Networks,” *Phys. Rev. Lett.* **110**, 028701 (2013).
- [11] Filippo Radicchi and Alex Arenas, “Abrupt transition in the structural formation of interconnected networks,” *Nat Phys* **9**, 717–720 (2013).
- [12] Marina Diakonova, Maxi San Miguel, and Víctor M. Eguíluz, “Absorbing and shattered fragmentation transitions in multilayer coevolution,” *Phys. Rev. E* **89**, 062818 (2014).
- [13] Naoki Masuda, “Voter model on the two-clique graph,” *Phys. Rev. E* **90**, 012802 (2014).
- [14] Arda Halu, Kun Zhao, Andrea Baronchelli, and Ginestra Bianconi, “Connect and win: The role of social networks in political elections,” *EPL* **102**, 16002 (2013).
- [15] Jesús Gómez-Gardeñes, Irene Reinares, Alex Arenas, and Luis Mario Floría, “Evolution of Cooperation in Multiplex Networks,” *Sci Rep* **2** (2012), 10.1038/srep00620.
- [16] Luo-Luo Jiang and Matjaž Perc, “Spreading of cooperative behaviour across interdependent groups,” *Sci. Rep.* **3** (2013), 10.1038/srep02483.
- [17] M. D. Santos, S. N. Dorogovtsev, and J. F. F. Mendes, “Biased imitation in coupled evolutionary games in interdependent networks,” *Sci. Rep.* **4** (2014), 10.1038/srep04436.
- [18] Lucia Valentina Gambuzza, Mattia Frasca, and Jesus Gomez-Gardeñes, “Intra-layer synchronization in multiplex networks,” arXiv:1407.3283 [nlin] (2014), arXiv: 1407.3283.
- [19] Santo Fortunato, “Community detection in graphs,” *Physics Reports* **486**, 75–174 (2010).
- [20] Peter J. Mucha, Thomas Richardson, Kevin Macon, Mason A. Porter, and Jukka-Pekka Onnela, “Community Structure in Time-Dependent, Multiscale, and Multiplex Networks,” *Science* **328**, 876–878 (2010).
- [21] Marya Bazzi, Mason A. Porter, Stacy Williams, Mark McDonald, Daniel J. Fenn, and Sam D. Howison, “Community detection in temporal multilayer networks, and its application to correlation networks,” arXiv:1501.00040 [nlin, physics:physics, q-fin] (2014), arXiv: 1501.00040.
- [22] Manlio De Domenico, Andrea Lancichinetti, Alex Arenas, and Martin Rosvall, “Identifying Modular Flows on Multilayer Networks Reveals Highly Overlapping Organization in Interconnected Systems,” *Phys. Rev. X* **5**, 011027 (2015).
- [23] Martin Rosvall and Carl T. Bergstrom, “Mapping Change in Large Networks,” *PLoS ONE* **5**, e8694 (2010).
- [24] P. Ronhovde, S. Chakrabarty, D. Hu, M. Sahu, K. K. Sahu, K. F. Kelton, N. A. Mauro, and Z. Nussinov, “Detecting hidden spatial and spatio-temporal structures in glasses and complex physical systems by multiresolution network clustering,” *Eur. Phys. J. E* **34**, 1–24 (2011).
- [25] Danielle S. Bassett, Mason A. Porter, Nicholas F. Wymbs, Scott T. Grafton, Jean M. Carlson, and Peter J. Mucha, “Robust detection of dynamic community structure in networks,” *Chaos: An Interdisciplinary Journal of Nonlinear Science* **23**, 013142 (2013).
- [26] Marta Sarzynska, Elizabeth A. Leicht, Gerardo Chow-

- ell, and Mason A. Porter, "Null Models for Community Detection in Spatially-Embedded, Temporal Networks," arXiv:1407.6297 [nlin, physics:physics, q-bio] (2014), arXiv: 1407.6297.
- [27] Laetitia Gauvin, André Panisson, and Ciro Cattuto, "Detecting the Community Structure and Activity Patterns of Temporal Networks: A Non-Negative Tensor Factorization Approach," PLoS ONE **9**, e86028 (2014).
- [28] Mel MacMahon and Diego Garlaschelli, "Community Detection for Correlation Matrices," Phys. Rev. X **5**, 021006 (2015).
- [29] Paul W. Holland, Kathryn Blackmond Laskey, and Samuel Leinhardt, "Stochastic blockmodels: First steps," Social Networks **5**, 109–137 (1983).
- [30] Stephen E. Fienberg, Michael M. Meyer, and Stanley S. Wasserman, "Statistical Analysis of Multiple Sociometric Relations," Journal of the American Statistical Association **80**, 51–67 (1985).
- [31] Katherine Faust and Stanley Wasserman, "Blockmodels: Interpretation and evaluation," Social Networks **14**, 5–61 (1992).
- [32] Carolyn J. Anderson, Stanley Wasserman, and Katherine Faust, "Building stochastic blockmodels," Social Networks **14**, 137–161 (1992).
- [33] Aaron Clauset, Christopher Moore, and M. E. J. Newman, "Hierarchical structure and the prediction of missing links in networks," Nature **453**, 98–101 (2008).
- [34] Tiago P. Peixoto, "Hierarchical Block Structures and High-Resolution Model Selection in Large Networks," Phys. Rev. X **4**, 011047 (2014).
- [35] Edoardo M. Airoldi, David M. Blei, Stephen E. Fienberg, and Eric P. Xing, "Mixed Membership Stochastic Blockmodels," J. Mach. Learn. Res. **9**, 1981–2014 (2008).
- [36] Brian Ball, Brian Karrer, and M. E. J. Newman, "Efficient and principled method for detecting communities in networks," Phys. Rev. E **84**, 036103 (2011).
- [37] Tiago P. Peixoto, "Model Selection and Hypothesis Testing for Large-Scale Network Models with Overlapping Groups," Phys. Rev. X **5**, 011033 (2015).
- [38] Brian Karrer and M. E. J. Newman, "Stochastic blockmodels and community structure in networks," Phys. Rev. E **83**, 016107 (2011).
- [39] Leto Peel and Aaron Clauset, "Detecting change points in the large-scale structure of evolving networks," arXiv:1403.0989 [physics, stat] (2014), arXiv: 1403.0989.
- [40] Toni Valles-Català, Francesco A. Massucci, Roger Guimera, and Marta Sales-Pardo, "Multilayer stochastic block models reveal the multilayer structure of complex networks," arXiv:1411.1098 [cond-mat, physics:physics] (2014), arXiv: 1411.1098.
- [41] Jonathan Q. Jiang, "Stochastic block model and exploratory analysis in signed networks," Phys. Rev. E **91**, 062805 (2015).
- [42] Pierre Barbillon, Sophie Donnet, Emmanuel Lazega, and Avner Bar-Hen, "Stochastic Block Models for Multiplex networks: an application to networks of researchers," arXiv:1501.06444 [stat] (2015), arXiv: 1501.06444.
- [43] Subhadeep Paul and Yuguo Chen, "Community detection in multi-relational data with restricted multi-layer stochastic blockmodel," arXiv:1506.02699 [stat] (2015), arXiv: 1506.02699.
- [44] Marco Corneli, Pierre Latouche, and Fabrice Rossi, "Exact ICL maximization in a non-stationary time extension of the latent block model for dynamic networks," arXiv:1506.04138 [stat] (2015), arXiv: 1506.04138.
- [45] Natalie Stanley, Saray Shai, Dane Taylor, and Peter J. Mucha, "Clustering Network Layers With the Strata Multilayer Stochastic Block Model," arXiv:1507.01826 [physics, stat] (2015), arXiv: 1507.01826.
- [46] Mahendra Mariadassou, Stéphane Robin, and Corinne Vacher, "Uncovering latent structure in valued graphs: A variational approach," Ann. Appl. Stat. **4**, 715–742 (2010).
- [47] Roger Guimerà and Marta Sales-Pardo, "A Network Inference Method for Large-Scale Unsupervised Identification of Novel Drug-Drug Interactions," PLoS Comput Biol **9**, e1003374 (2013).
- [48] Núria Rovira-Asenjo, Tània Gumí, Marta Sales-Pardo, and Roger Guimerà, "Predicting future conflict between team-members with parameter-free models of social networks," Sci. Rep. **3** (2013), 10.1038/srep01999.
- [49] Christopher Aicher, Abigail Z. Jacobs, and Aaron Clauset, "Learning latent block structure in weighted networks," jcomplexnetw , cnu026 (2014).
- [50] Tianbao Yang, Yun Chi, Shenghuo Zhu, Yihong Gong, and Rong Jin, "Detecting communities and their evolutions in dynamic social networks—a Bayesian approach," Mach Learn **82**, 157–189 (2010).
- [51] Kevin S. Xu and Alfred O. Hero III, "Dynamic Stochastic Blockmodels: Statistical Models for Time-Evolving Networks," in *Social Computing, Behavioral-Cultural Modeling and Prediction*, Lecture Notes in Computer Science No. 7812, edited by Ariel M. Greenberg, William G. Kennedy, and Nathan D. Bos (Springer Berlin Heidelberg, 2013) pp. 201–210.
- [52] K.S. Xu and A.O. Hero, "Dynamic Stochastic Blockmodels for Time-Evolving Social Networks," IEEE Journal of Selected Topics in Signal Processing **8**, 552–562 (2014).
- [53] Kevin S. Xu, "Stochastic Block Transition Models for Dynamic Networks," arXiv:1411.5404 [physics, stat] (2014), arXiv: 1411.5404.
- [54] Amir Ghasemian, Pan Zhang, Aaron Clauset, Christopher Moore, and Leto Peel, "Detectability thresholds and optimal algorithms for community structure in dynamic networks," arXiv:1506.06179 [cond-mat, physics:physics, stat] (2015), arXiv: 1506.06179.
- [55] Tiago P. Peixoto, "Entropy of stochastic blockmodel ensembles," Phys. Rev. E **85**, 056122 (2012).
- [56] Peter D. Grünwald, *The Minimum Description Length Principle* (The MIT Press, 2007).
- [57] Jorma Rissanen, *Information and Complexity in Statistical Modeling*, 1st ed. (Springer, 2010).
- [58] Martin Rosvall and Carl T. Bergstrom, "An information-theoretic framework for resolving community structure in complex networks," PNAS **104**, 7327–7331 (2007).
- [59] Tiago P. Peixoto, "Parsimonious Module Inference in Large Networks," Phys. Rev. Lett. **110**, 148701 (2013).
- [60] E. T. Jaynes, *Probability Theory: The Logic of Science*, edited by G. Larry Bretthorst (Cambridge University Press, Cambridge, UK ; New York, NY, 2003).
- [61] Sir Harold Jeffreys, *The Theory of Probability* (Oxford University Press, 1998).
- [62] Tiago P. Peixoto, "Efficient Monte Carlo and greedy heuristic for the inference of stochastic block models," Phys. Rev. E **89**, 012804 (2014).
- [63] Aurelien Decelle, Florent Krzakala, Christopher Moore, and Lenka Zdeborová, "Asymptotic analysis of the stochastic block model for modular networks and its al-

- gorithmic applications,” Phys. Rev. E **84**, 066106 (2011).
- [64] Florent Krzakala, Christopher Moore, Elchanan Mossel, Joe Neeman, Allan Sly, Lenka Zdeborová, and Pan Zhang, “Spectral redemption in clustering sparse networks,” PNAS , 201312486 (2013).
- [65] Tiago P. Peixoto, “The graph-tool python library,” figshare (2014), 10.6084/m9.figshare.1164194.
- [66] Aurelien Decelle, Florent Krzakala, Christopher Moore, and Lenka Zdeborová, “Inference and Phase Transitions in the Detection of Modules in Sparse Networks,” Phys. Rev. Lett. **107**, 065701 (2011).
- [67] James Coleman, Elihu Katz, and Herbert Menzel, “The Diffusion of an Innovation Among Physicians,” Sociometry **20**, 253–270 (1957).
- [68] D. Holten, “Hierarchical Edge Bundles: Visualization of Adjacency Relations in Hierarchical Data,” IEEE Transactions on Visualization and Computer Graphics **12**, 741–748 (2006).
- [69] Julie Fournet and Alain Barrat, “Contact Patterns among High School Students,” PLoS ONE **9**, e107878 (2014).
- [70] Naoki Masuda, Konstantin Klemm, and Víctor M. Eguíluz, “Temporal Networks: Slowing Down Diffusion by Long Lasting Interactions,” Phys. Rev. Lett. **111**, 188701 (2013).
- [71] Valerio Gemmetto, Alain Barrat, and Ciro Cattuto, “Mitigation of infectious disease at school: targeted class closure vs school closure,” BMC Infectious Diseases **14**, 695 (2014).
- [72] Nicolas Voirin, Cécile Payet, Alain Barrat, Ciro Cattuto, Nagham Khanafer, Corinne Régis, Byeul-a Kim, Brigitte Comte, Jean-Sébastien Casalegno, Bruno Lina, and Philippe Vanhems, “Combining High-Resolution Contact Data with Virological Data to Investigate Influenza Transmission in a Tertiary Care Hospital,” Infection Control & Hospital Epidemiology **36**, 254–260 (2015).